INVESTIGATION OF NONSTATIONARY CONDITIONS OF OPTICAL FIBER FORMATION. III. DRAWING PROCESS REACTION UNDER THERMAL ACTIONS AND PERTURBATIONS OF THE BLANK RADIUS

V. N. Vasil'ev, G. N. Dul'nev, and V. D. Naumchik

UDC 532.522:681.7.068.4

Results are represented of numerical computations for the blank radius perturbation, the furnace temperature, and the coefficient of external heat elimination and general deductions are formulated in the investigation of nonstationary drawing conditions.

Problems on the stability of the drawing process and the reaction of the optical fiber (OF) radius under perturbations in the supply and drawing rates were examined in the first and second parts of the research [1, 2]. Fluctuations in the blank radius R_0, the furnace temperature T_p, and the external heat elimination coefficient are among the other kinds of perturbing actions that can be examined within the framework of a quasi-one-dimensional mathematical model [3, 4]. Investigation of the process reaction under the mentioned external actions was performed totally on the basis of the algorithm elucidated in [2]. The initial data for the computations and the notation, unless mentioned especially here, correspond to that presented in [2].

I. Perturbation of the Radius of the Initial Blank. The regularities, remarked in [2], for the change in R_B and F_f in time during fluctuations of the supply rate are also valid for this case (Figs. 1 and 2). Attention must be turned to the following:

1) out of all the cases of perturbing actions considered, the linear approximation is most adequate for the nonlinear mathematical model to describe blank radius perturbations (Fig. 1);

2) the OF drawing process reaction to the perturbation R_0 significantly exceeds (by two-three times) its reaction to the perturbation V_B and V_0 (Fig. 2);

3) the temperature conditions for fiber formation have negligible influence on the amplitude-frequency characteristic (AFC) in high-speed drawing (Fig. 2, see curves 4 and 5 for comparison).

II. Perturbation of the Furnace Temperature and External Heat Elimination Coefficient. Results of computing the transfer function and AFC for perturbation of the furnace temperature and the external heat elimination coefficient from the jet surface are presented in Figs. 3-5. The following deductions can be drawn from a consideration of the graphs presented.

The system reaction to the perturbation T_p is quite definitely nonlinear in nature. This latter appears especially clearly in the radical difference in the behavior of the transfer function under positive and negative actions (Fig. 3, curves 1 and 3). Satisfactory correspondence (the discrepancy does not exceed 20%) between the linear and nonlinear model is observed for a magnitude of the action less than 15-20°C. The essential distinction between the results of experiments and computation can apparently be referred to inertia of furnace heating, i.e., to the impossibility of reproducing a stepwise rise in temperature under experimental conditions. The validity of this assertion is confirmed by the presence of the section with ΔR_B practically equal to zero on the curve 6 (Fig. 3) for $\tau < 2$—3 sec.

Analogously to the perturbations V_0, V_B, R_0 examined above, a substantial diminution in the amplitude of the fluctuating motion is observed as the drawing rate increases (Figs. 3-5), and the appearance of high-frequency fluctuations (Fig. 5, curve 3 and 5) is possible during overheating of the glass mass melt. In conclusion, it must be noted that the reaction of the OF drawing process to the perturbation T_p substantially exceeds (up to ten times) its reaction to the perturbation R_0, V_B, V_0 and the change in the fiber radius is the most insignificant out of all the cases considered for some fluctuations of the number St (Fig. 3, curve 7 and Fig. 5, curve 6).

III. Experimental investigations of the OF drawing process (see [5], say) showed the presence of frequencies to 100 Hz in the fiber exit diameter fluctuation spectrum. The presence of correlation between the drawing equipment vibrations and the R_B fluctuations is noted here. The numerical investigation performed for the nonstationary processes permits the assertion that high-frequency fluctuations in the supply and drawing rates, the blank radius, the furnace

Leningrad Institute of Precision Mechanics and Optics. Translated from Inzhenerno-Fizicheskii Zhurnal, Vol. 58, No. 3, pp. 499-505, March, 1990. Original article submitted September 15, 1988.

 0022-0841/90/5803-0370$12.50

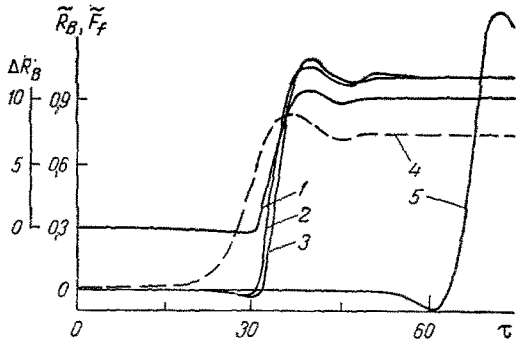

Fig. 1. Change in the radius during step-wise perturbation of the blank radius (1 is the solution of the nonlinear system of equations and 2-5 are the solution of the linearized equations): 1) T_{p_2} = 2250°C, V_B = 10 m/sec, F_f = 0.186 N, perturbation magnitude 10%; 2) 2250, 10, 0.186, 10; 3) 2150, 10, 0.388, 10; 4) perturbation F_f for 2; 5) 2250, 3, 0.19, 10. ΔR_B, μm; R_B, F_f, %.

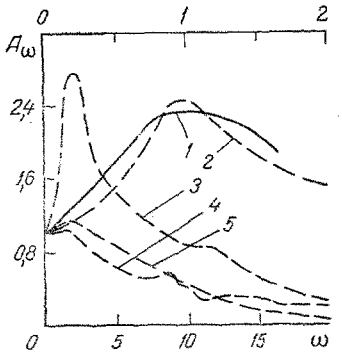

Fig. 2. Amplitude-frequency characteristic (AFC) under radius perturbations: 1) T_{p2} = 2250°C, V_B = 3 m/sec; 2) 2250, 3; 3) 2250, 0.5; 4) 2250, 10; 5) 2150, 10 (upper scale for 1-3, lower for 4, 5; solid line is AFC computation on the basis of solving the system of differential equations [2], dashed are for Fourier-weight function transformation; ω is the number of fluctuations in 2π sec).

temperature, and the external heat elimination coefficient are filtered out by the deformation zone (above 0.5 Hz for V_B < 1 and 6.5 Hz for V_B = 10 m/sec). Therefore, it is impossible to refer the presence of high-frequency R_B fluctuations to any of the perturbing actions considered above.

The drawing equipment vibrations can result in not only fluctuations in V_B, V_0, and St but also in a change in the radiant thermal flux distribution over the melt surface with the lapse of time. If the vibrational motion is decomposed into longitudinal and transverse components, then the transverse fluctuations will result in disturbance of the axial symmetry of the heating, and the longitudinal in fluctuations of the radiant heat flux along the length of the deformation zone.

Within the framework of a one-dimensional model of the OF drawing process the longitudinal vibrations of the drawing equipment can be modelled if it is assumed in the energy equation [3] that the integral term (it determines the radiant thermal flux from the furnace surface) equals

$$Q(x) = \frac{4n_c^2 \sigma_0 R_p (R_p - R)}{R}$$

$$\times \int_{\delta\sin(\omega\tau)}^{1+\delta\sin(\omega\tau)} \frac{\{\beta\varepsilon_p T_p^4 [\eta - \delta \sin(\omega\tau)] - \varepsilon T^4\} [R_p - R + kR'(x-\eta)]}{[(\eta - x)^2 + (R_p - R)^2]^2} d\eta.$$

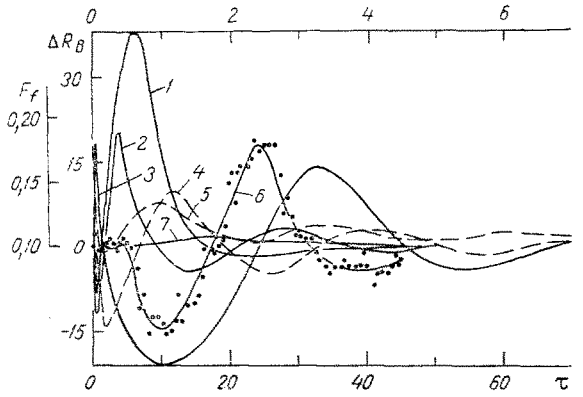

Fig. 3. Change in OF radius under stepwide perturbation of the furnace temperature and the number St (solution of the nonlinear system of equations: 1) T_{p2} = 2250°C, ξ = 0.375, R_p = 0.01 m, F_f = 0.011 N, R_0 = 0.005 m, R_B = 64 μm, V_B = 0.5 m/sec, perturbation magnitude equals +2%; 2) 2350, 0.565, 0.015, 0.019, 0.0046, 62.5, 3, 2; 3) drawing conditions correspond to 1, magnitude of the perturbation is 2%; 4) 2250, 0.375, 0.01, 0.186, 0.005, 64, 10, 12; 5) perturbation F_f for 4; 6) experimental values, T_p = 2320°C, R_p = 0.015, F_f = 0.025 N, R_0 = 0.0046 m, R_B = 62.5 μm, V_B = 3 m/sec, perturbation magnitude +2%; 7) drawing conditions correspond to 1, perturbation St = 30% (lower scale for 1-3, 6, 7; upper for 4, 5; points are experimental values for 6) F_f, N; τ, sec.

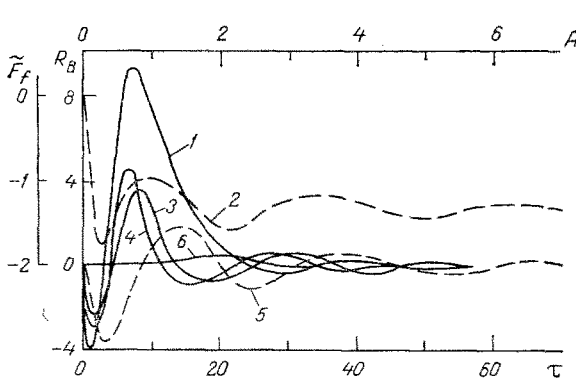

Fig. 4

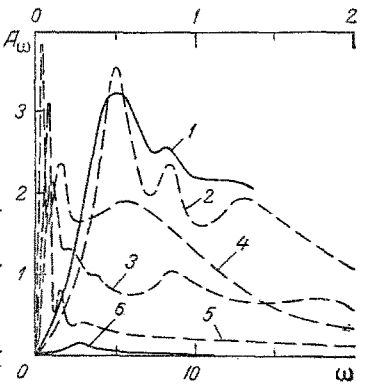

Fig. 5

Fig. 4. Change in OF radius under stepwise perturbation of the furnace temperature and external heat elimination coefficient (solution of the linearized system of equations): 1) T_{p2} = 2250°C, V_B = 0.5 m/sec, perturbation magnitude 0.5%; 2) perturbation F_f for 5; 3) 2250, 3, 0.5; 4) 2150, 3, 0.5; 5) 2250, 10, 0.5; 6) T_{p2} = 2250°C, V_B = 0.5 m/sec, perturbation St = 5% (lower scale for 1, 3, 4, 6; upper for 2, 5).

Fig. 5. Amplitude-frequency characteristics (AFC) of OF drawing process under perturbation of the furnace temperature and external heat elimination coefficient: 1) T_{p2} = 2250°C, V_B = 3 m/sec; 2) 2250, 3; 3) 2250, 0.5; 4) 2250, 0.5; 5) 2150, 10; 6) 2250, 0.5, perturbation St (upper scale for 1, 2, 4, 6; lower for 3, 5; solid lines, solution of differential equations; dashes, Fourier-weight function transformation; ω, number of fluctuations in 2π sec).

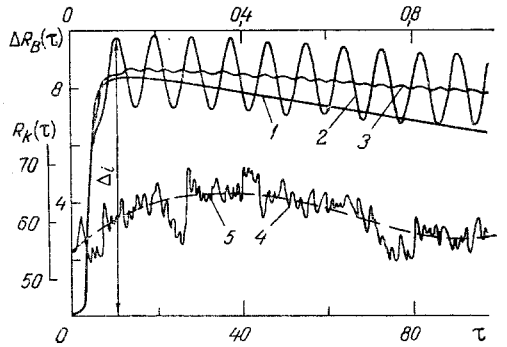

Fig. 6. Change in the fiber radius in time for longitudinal furnace vibrations (T_{p2} = 2250°C, V_B = 0.5 m/sec, δ = 400 μm): 1) ω = 50 Hz; 2) 0.1; 3) 10; 4) results of experiment, V_B = 1 m/sec; 5) low-frequency component for 4 (upper scale for 1-3; lower for 4, 5; Δ_i, amplitude of the first harmonic). R_B, μm.

TABLE 1. Dependence of the First Harmonic Amplitude of the Function ΔR_B on ω and δ for Longitudinal Furnace Vibrations (T_{p_2} = 2250°C, V_B = 0.5 m/sec)*

δ	ω				
	0,628	6,28	62,8	125,6	314
50	8,532	8,376	8,705	8,633	8,599
100	8,512	8,270	8,862	8,815	8,562
400	8,411	7,827	9,823	9,228	8,625
2000	8,082	6,721	15,564	12,614	9,683

*Here ω is the number of vibrations in 2π sec; ΔR_B, δ, μm.

Physically this means that at a certain time $\tau = 0$ the heating unit starts to perform longitudinal fluctuations with amplitude δ and circular frequency ω relative to the fixed blank, whereupon there will be a periodic change in the radiant thermal flux distribution to the surface of the deformation domain.

The dependence of the amplitude of the first harmonic Δ_i (see Fig. 6) on ω and δ is represented in the table. The quantity Δ_i is chosen as the characteristic of this perturbing action since it is not expedient to continue the calculation until system emergence in the quasistationary mode because of the large computation time for this problem since the magnitude of the first harmonic is evidently a certain measure of this state. A deduction can be drawn from examination of the table that the function ΔR_B has two maximums (low-frequency in the 0.08-0.12 Hz range and high-frequency in the 8-12 Hz range) while the longitudinal furnace vibrations can result in fiber radius perturbation even for ω = 50 Hz (for instance, ΔR_B is a quantity about 8 μm for δ = 50-2000 μm at the frequency 50 Hz).

The nature of the change in ΔR_B in time (Fig. 6) permits noting the following regularities.

furnace vibrations at a frequency less than 1-3 Hz result in low-frequency fluctuations of the fiber radius at a frequency 0.01-0.01 Hz whose amplitude depends on the specific value of ω and δ (see Table 1);

for a furnace vibration frequency greater than 5 Hz a certain low-frequency component (0.01-0.1 Hz) can be extracted in the graph of the function ΔR_B, on which a high-frequency component is superposed (Fig. 6, curves 1 and 3); the maximum of the secondary vibration amplitudes is observed at a frequency of the order of 10 Hz.

From the physical viewpoint this change in the fiber radius in time is caused by radiation thermal flux fluctuations along the whole surface of the deformation domain (Fig. 7, curves 4-7), that results in periodic fluctuations in the melt temperature and is the reason for fiber radius perturbation. An approximate agreement between the temperature fluctuation frequency at some point of the melt and ΔR_B is observed here. The difference, in principle, between the furnace vibrational motion along the blank surface and the change in its temperature is that only the magnitude of the deliverable thermal flux in the middle part of the deformation domain fluctuates in the latter case without a change in the nature of its distribution along the jet surface (see Fig. 7, curves 1-3).

Shown in combination with the results of a computation in Fig. 6 is an experimental graph (measurements are performed for a deflected control system) in which a certain high- and a low-frequency component of the function R_B

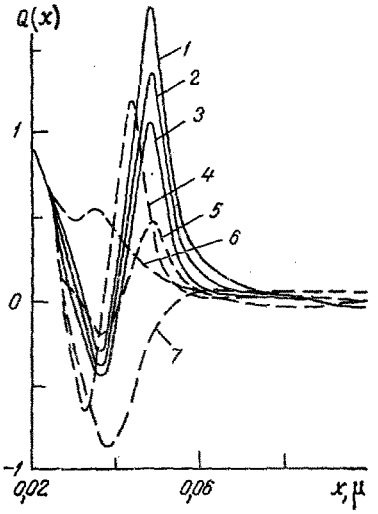

Fig. 7. Distribution of the resultant radiation flux along the length of the deformation domain for longitudinal furnace vibrations (V_B = 3 m/sec, δ = 0.002 m, ω = 1 Hz): 1) T_{p2} = 2250; 2) 2150; 3) 2050; 4) T_{p2} = 2150°C, τ = 0.026; 5) 2150, 0.0726; 6) 2150, 0.571; 7) 2150, 0.226 (solid lines are stationary mode, dashes are nonstationary mode).

(see Fig. 5) can be extracted analogously to that considered above. On the basis of comparing the presented results, the assumption can be made that this nature of the change in fiber radius in time can be explained by the existence of high-frequency thermal flux fluctuation at the surface of the deformation domain. Vibrations of the drawing equipment, resulting in disturbance of the heating symmetry and stationary conditions, say, can be a source of this perturbing action. IV. In conclusion, the following deductions can be made by summarizing the numerical investigation performed for the nonstationary OF formation conditions:

1. Comparison of the computed and experimental data showed the adequacy of the developed mathematical model for an OF drawing process as well as the possibility of describing the nonstationary OF formation conditions by a linearized system of governing equations when the amplitude of the perturbing action is less than 1% of the nominal value of the parameter.

2. Construction of the AFC on the basis of the Fourier-weight function transformation yields more preferable results since the computation time is shortened substantially (two-three times).

3. Stability of the melt flow in the deformation zone depends most essentially on the velocity coefficient, the temperature regime of the formation, and the drawing rate. It is noted first that an increase in V_B and the glass mass temperature (within specific limits) results in an increase in drawing stability for W = const; here:

a) less stable regimes of fiber formation have a higher amplitude of vibrational motion near the equilibrium position;

b) an increase in the drawing rate results in shortening of the transient time, a substantial diminution in the amplitude of the R_B fluctuations, and the function R_B becomes practically aperiodic for V_B = 10 m/sec;

c) a rise in the melt temperature results in diminution of the amplitude of the first harmonic; however, under these conditions the origination of secondary high-frequency vibrations is possible.

4. A kind of perturbing action can be determined from the nature of the change in the tensile force in initial time segments (τ < 1 sec). For τ > 1 sec the F_f starts to perform synchronized vibrations with R_B, leading the latter somewhat in phase.

5. For any kind of perturbing action the amplitude of the first AFC peak is determined by the temperature and the velocity coefficient, and its position on the frequency scale by the drawing rate.

6. The perturbing actions examined above can be arranged in the following order according to the growth in the level of their significance: the perturbation of the external heat elimination coefficient, the drawing delivery rate, the radius of the initial blank, and the furnace temperature. The reaction of the drawing process to the R_0 and T_p fluctuations exceeds its reaction for V_0, V_B, St perturbations by 2-10 times. The OF formation process possesses the least inertia during different changes in the drawing rate; consequently, control in this channel is most efficient.

7. For any kind of perturbing action for V_B < 1 m/sec, all vibrations with a frequency greater than 0.5 Hz are filtered in the deformation domain, and frequencies above 6.5 Hz for V_B = 10 m/sec. In all cases the AFC maximum

is in the 0.1-1 Hz band; consequently, attention must especially be turned to stabilization of the furnace temperature and the blank radius at the low frequencies since the reaction of the OF drawing process is most substantial for this kind of drawing process.

8. Heating of the glass mass melt results in formation of high-frequency vibrations; consequently it is inexpedient to raise the temperature in the deformation domain above 1950-2050°C for $V_B < 1$ m/sec and 2200°C for $V_B = 10$ m/sec.

9. The presence of a section with $T_p = \text{const}$ is not desirable in the temperature distribution along the heating element surface since this results in the appearance of a certain volume of glass at a practically constant temperature in the deformation domain. This latter results in diminution of the stability of the drawing process and an increase in its reaction to external perturbations since the formation conditions are shifted substantially towards the isothermal.

10. It is shown that the experimentally noted high-frequency fiber radius fluctuations can be among the high-frequency radiation thermal flux fluctuations at the blank surface that appear because of disturbance of the heating symmetry and stationary conditions.

11. On the basis of the results presented, it can be concluded that the main factors governing the stability of melt flow in the deformation zone and the nature of progress of transients are the temperature conditions for blank heating. Its certain specific melt temperature distribution exists for each value of W and V_B, that yields maximal stability and minimal reaction to the external perturbing actions of the drawing process.

NOTATION

R_0, blank radius; V_B, drawing rate; V_0, delivery rate; T_p, furnace temperature; R_B, fiber radius; τ, time; n_c, gas refractive index; σ_0, Stefan—Boltzmann constant; R_p, furnace radius; R, jet radius; β, absorption coefficient; ε_p, furnace surface emissivity; η, variable of integration; ε, melt emissivity; T, melt temperature; x, coordinate; F_f, tensile force; T_{p2}, ξ parameters governing the temperature distribution along the heater surface; $W = V_B/V_0$, velocity coefficient; $St = h/\rho V_0 l$, Stanton number; h, coefficient of external heat elimination; ρ, melt density; l, length of the computational domain; k, weight factor; $\Delta R_B = R_B(\tau) - R_B$; $(...)' = d/dx$.

LITERATURE CITED

1. V. N. Vasil'ev, G. N. Dul'nev, and V. D. Naumchik, Inzh.-Fiz. Zh., 55, No. 2, 284-292 (1988).
2. V. N. Vasil'ev, G. N. Dul'nev, and V. D. Naumchik, Inzh.-Fiz. Zh., 58, No. 2, 288-296 (1990).
3. V. D. Naumchik, Energy Transport in Convective Flows [in Russian] (Collection of Scientific Research, Inst. of Heat and Mass Transfer, BSSR Acad. of Sci.), 39-63 (1985).
4. V. N. Vasil'ev and V. D. Naumchik, Prikl. Mekh. Tekh. Fiz., No. 2, 77-84 (1988).
5. R. E. Jaeger, Fiber Optics Advances in Research and Development, 33-64 (1985).